FUS Mutation Causes Disordered Lipid Metabolism in Skeletal Muscle Associated with ALS

Binbin Zhou[1,2] · Yilei Zheng[1] · Xiaobing Li[1] · Huifang Dong[1] · Jiaxi Yu[2] · Yang Zou[4] · Min Zhu[1] · Yanyan Yu[1] · Xin Fang[1] · Meihong Zhou[1] · Wei Zhang[2] · Yun Yuan[2] · Zhaoxia Wang[2,3] · Jianwen Deng[2,3] · Daojun Hong[1,5]

Abstract

Amyotrophic lateral sclerosis (ALS) is a devastating neurodegenerative disease characterized by dysfunction of the upper and lower motor neurons resulting in muscle weakness and wasting. Recently, several studies on ALS patients and ALS animal models indicated that intramuscular toxicity played a role in ALS disease progression; however, the mechanisms driving this are unknown. In this study, we explored the possible dysfunction of lipid metabolism in myocytes associated with ALS. Initially, skeletal muscle from 41 ALS patients, as well as 53 non-ALS control subjects, was investigated, and we identified that lipid droplet accumulation in the muscle fibers of ALS patients was significantly increased, especially in patients with *FUS* mutations. A myoblast (C2C12) cell line expressing mutant FUS (FUS-K510Q) was able to induce lipid droplet accumulation and mitochondrial dysfunction. Consistently, transgenic flies expressing FUS-K510Q under a muscle-specific driver showed elevated triglyceride levels in the flight muscles, as well as locomotor defects. Biochemical analysis of C2C12 cells and fly muscle tissues showed upregulation of PLIN2, and downregulation of ATGL and CPT1A, indicating inhibition of lipolysis and fatty acid β-oxidation in muscle cells with *FUS* mutations. Our study provided a potential explanation for the pathogenesis associated with lipid droplets accumulating in skeletal muscle in ALS. Our data also suggested that disordered lipid metabolism and mitochondrial dysfunction play a crucial role in intramuscular toxicity in ALS.

Keywords Fused in sarcoma · Amyotrophic laterals sclerosis · Skeletal muscle · Lipid metabolism · Mitochondrial dysfunction

---

Binbin Zhou and Yilei Zheng contributed equally as co-first authors.

✉ Zhaoxia Wang
   drwangzx@163.com

✉ Jianwen Deng
   jianwendeng@pkufh.com

✉ Daojun Hong
   hongdaojun@hotmail.com

1   Department of Neurology, the First Affiliated Hospital of Nanchang University, Nanchang 330006, China

2   Department of Neurology, Peking University First Hospital, Beijing 100034, China

3   Beijing Key Laboratory of Neurovascular Disease Discovery, Beijing 100034, China

4   Department of Cardiology, Jiangxi Provincial People's Hospital Affiliated to Nanchang University, Nanchang, Jiangxi Province, China

5   Department of Medical Genetics, the First Affiliated Hospital of Nanchang University, Nanchang 330006, China

Introduction

Amyotrophic lateral sclerosis (ALS) is a fatal neurodegenerative disease characterized by aggressive degeneration of anterior horn neurons, brainstem neurons, and the corticospinal tract [1]. About 90% of cases are sporadic ALS (SALS) and the remaining 10% are familial ALS (FALS) [2]. At present, the onset of ALS is observed mostly in adulthood. The peak age is 47–52 years old in patients with familial ALS, and 58–63 years old in patients with sporadic ALS, while the patients with mutations in the fused in sarcoma (*FUS*) gene typically have juvenile onset. Typical clinical symptoms of ALS include limb weakness, muscle wasting, bulbar paralysis, and respiratory insufficiency, which lead to death 3–5 years after disease onset [3].

There are more than 30 known disease-causing genes for ALS, including *FUS*, Cu/Zn superoxide dismutase 1 (*SOD1*), TAR DNA-binding protein 43 (*TARDBP*), valosin containing protein (*VCP*), and chromosome 9 open reading

frame 72 (*C9ORF72*) [2, 3]. *FUS* gene is the most common causative gene in sporadic juvenile ALS patients in China and has become a research hotspot in recent years. Previous studies have shown that *FUS* mutations can lead to abnormal cytoplasmic localization and formation of inclusion bodies, resulting in motor neuron loss associated with neurotoxicity. Skeletal muscle lesions used to be considered secondary neurogenic effect after motor neuron loss [4, 5]. However, a recent study on induced pluripotent stem cell (iPSC)-derived myotubes and motor neurons of patients with ALS-FUS has shown toxicity in both motor neurons and muscles [6]. Additionally, abnormalities in mitochondrial function and lipid metabolism may appear during pathological assessment of biopsied muscle tissue in most patients with ALS, which further suggests that *FUS* mutations may cause toxicity to skeletal muscle [7].

Under physiological conditions, lipid droplets act as storage for neutral lipids in cells. Triglyceride hydrolases (ATGL) on the surface of lipid droplets is responsible for hydrolyzing triglycerides into diglycerides and free fatty acids. As such, ATGL is the first rate-limiting enzyme in the lipolysis pathway [8]. When the lipolysis pathway is blocked, it may be compensated for by enhancement of selective lipid autophagy metabolism [9]. In studies of transgenic mouse models expressing *SOD1* or *TARDBP* mutations, it was found that muscle fibers were more dependent on fatty acid while glucose uptake was decreased, suggesting that dysregulated lipid metabolism may be involved in the pathogenesis observed in ALS patients with *SOD1* or *TARDBP* mutation [10, 11]. Our previous study found that mutant FUS protein can impair the assembly and function of mitochondrial ATP synthases in cellular and transgenic fly models, leading to mitochondrial dysfunction and neuronal cell death [12]. Moreover, pathological studies have found that in muscle biopsies of patients with ALS, lipid droplets accumulated significantly in muscle cells [7]. However, in FUS-ALS skeletal muscle, the molecular mechanisms driving lipid metabolism dysfunction and mitochondrial damage are still unclear.

Herein, we systematically examined lipid droplet accumulation in muscle biopsies from ALS patients. ALS-related FUS-K510Q mutant was expressed in a myoblast (C2C12) cellular model [13, 14] and a transgenic fly model to investigate the mechanisms involved in disordered lipid metabolism and mitochondrial dysfunction in muscle cells.

Materials and Methods

Subjects

All patients in this study were diagnosed with definite or probable ALS according to EI criteria [15] and were enrolled in the Department of Neurology at the First Affiliated Hospital of Nanchang University and the Peking University First Hospital from January 2010 to December 2018. Additionally, subjects initially suspected of myopathy but without any abnormal pathological changes detected in their muscle biopsy were used as controls. Control subjects' gender and age were well matched with ALS patients. All clinical materials used in this study were obtained for diagnostic purposes with written informed consent. This study was approved by the Ethics Committee of the First Affiliated Hospital of Nanchang University and the Peking University First Hospital.

Muscle Pathological Examination

Muscle biopsies were performed on the affected limb in all patients. The muscle tissue was frozen and then cut into 8-μm sections. These sections were stained with standard histological and enzyme histochemical procedures as in our previous study [7]. The muscle biopsy specimens were pathologically stained at different hospitals at different time points, which were related to the patient's first visit. To a certain extent, muscle pathological staining may have different chromatic aberrations when viewed by light microscope.

Genetic Testing

Genomic DNA was extracted from peripheral blood samples. Whole-exome sequencing (WES) was commercially supported by Running Gene Inc. (Beijing, China). In brief, multiple neurodegenerative genes, including known ALS genes (SOD1, ALS2, SETX, FUS, VAPB, ANG, TARDBP, FIG 4, OPTN, VCP, UBQLN2, KIF5A, TIA1, ANXA11, SIGMAR1, CHMP2B, PFN1, C9ORF72, ATXN2, AR, DCTN1, NEFH, PRPH, DAO, TFG, TAF15, and GRN), were analyzed. Hexanucleotide repeat expansion in C9orf72 was monitored by repeat-primed polymerase chain reaction (RP-PCR) according to the literature [16]. Mutations were named according to the HGVS nomenclature. A total of 41 ALS patients underwent whole-exome sequencing.

Cell Culture and Transfection

C2C12 cells were cultured in DMEM (BI) supplemented with 10% fetal bovine serum (FBS) (BI), and 100 unit/ml penicillin-streptomycin in a humidified incubator at 37°C under 5% CO_2/95% air. C2C12 cells were transfected with either Ctr (empty vector), Wt (full length of wild-type FUS protein), or FUS-K510Q mutant (full length of FUS-K510Q mutant protein) plasmids. For oleic acid treatment, cells were expressing Ctr, Wt, or FUS-K510Q for 24 h, and then 0.25 mM oleic acid was added to continue the culture for 24 h after treatment [13, 14]. The adenovirus AdMax

system (Vigenebio) was used for transduction according to the manufacturer's instructions.

Cell Viability Assays

Cell viability was measured using the CellTiter-Glo® (CTG) luminescent cell viability assay (Promega, WI, USA). Cells were seeded in white 6-well flat bottom plates and then treated with adenovirus transfection the following day. Luminescence was measured using a BioTek Synergyce Hybrid Microplate Reader (BioTek, VT, USA).

Fly Strains and Antibodies

Generation of transgenic flies expressing the human protein K510Q-FUS was described previously [16]. Mef2-Gal4 and Tubulin-Gal80^{ts} (Tub-Gal80^{ts}) were kindly provided by Dr. Tao Wang (National Institute of Biological Sciences). For flies under the Mef2-Gal4/Tub-Gal80^{ts}-driver, parental flies were crossed and cultured at 18°C, young flies after eclosion were transferred to 28°C for 4 h every day to induce FUS-K510Q expression [17–19]. Other flies were all cultured at 25°C. All flies were raised on standard fly food, 50% relative humidity, and 12-h–12-h light-dark cycles as described previously [20].

Antibodies used in this study include polyclonal rabbit-antibodies against FUS, CPT1A, PLIN2, and ATGL (ProteinTech Group Inc.), as well as a mouse monoclonal antibody anti-β-actin (ProteinTech Group Inc.).

Fly Motility Assay

The motility of adult flies expressing control or FUS-K510Q mutant were determined by using a modified climbing assay described in a previous study [21]. Briefly, 35-day-old flies were collected in each group. Fly climbing ability was examined as the number of flies climbing above a 3-cm line in 20 s after they were tapped to the bottom of an empty vial. The experiment was repeated 6 times for each group.

Fluorescence Microscopy

C2C12 cells were rinsed with 1X PBS and then fixed with 4% polyformaldehyde in 1×PBS after expression of GFP (Ctr) or K510Q FUS-EGFP for 48 h. The samples were mounted using prolong gold antifade mounting medium with DAPI (Invitrogen). Images were acquired at 60 × magnification by using a confocal microscope (Nikon A1MP).

Oil Red O staining

Slides were fixed with a 4% paraformaldehyde (PFA) solution for 20 min and then placed in ORO solution for 25 min,

rinsed with distilled water for 5 min, and counterstained with Mayer's hematoxylin (C0157S, Beyotime) for 5 min. The slides were then cover slipped with glycerin and observed by light microscopy (Nikon), where myocytes were photographed at 20× and 40×. Image analysis was performed with Image Pro Plus 6 software to calculate the lipid droplet ratio (the total area of red fat droplets accounted for the percentage of the entire ×20 image area used). The lipid droplet area ratio was calculated and averaged by two investigators [22, 23].

Measurement of Mitochondrial Membrane Potential by TMRM

Mitochondrial membrane potential was measured in cells expressing control vector or K510Q mutant FUS using tetra-methylrhodamine methyl ester (TMRM) (Invitrogen) following a published protocol [20]. Briefly, cells were rinsed in warm PBS and then stained using TMRM (40nM) for 20 min at 37°C. After 2 washes, the images were captured by an inverted research microscope ECLIPSE Ti2-E (Nikon). Fluorescent images were processed and quantified using Image J.

Mitochondrial ROS Detection Assay

Cells expressing control vector or K510Q mutant FUS for 48 h were rinsed in PBS and then stained with 10μM Dihydro-ethidium (DHE) for 30 min at 37°C. After washes, cells were fixed with 4% PFA for 10 min at room temperature. The images were captured by an inverted research microscope ECLIPSE Ti2-E (Nikon), and images were processed and quantified using ImageJ.

Measurement of Total Cellular ATP Levels

ATP levels were detected using a rapid bioluminescent ATP assay Kit (S0026, Beyotime Corporation). The measurement was performed according to the manufacturer's instructions. Briefly, C2C12 cells expressing either control vector or K510Q mutant FUS were seeded into 96-well plates. Following removal of the culture media, cell lysis with reaction mixtures was transferred to another opaque 96-well plate to measure luminescence. Luminescent signal values were normalized by the protein amount in each group to determine the total cellular ATP levels.

Measurement of the Triglyceride Levels

Triglyceride levels were detected using a GPO-PAP assay Kit (A110-1-1, Nanjing Jiancheng Institute of Biological Engineering). The measurement was performed according to the manufacturer's instructions.

Western Blot Analysis

Thoracic flight muscles from flies, as well as cultured cells, were lysed in RIPA buffer (50 mM Tris-HCl, pH 8.0, 150 mM NaCl, 0.25% sodium deoxycholate, 0.1% SDS, 1% NP-40, supplemented with complete protease inhibitor mixture; Roche). Lysates were assessed using Western blotting with the appropriate antibodies: anti-FUS (1:1000, Rabbit, Proteintech, # 11570-1-AP), anti-CPT1A (1:1000, Rabbit, Proteintech, #15184-1-AP), anti-ATGL (1:1000, Rabbit, Proteintech, #55190-1-AP), and anti-PLIN2 (1:1000, Rabbit, Proteintech, #15294-1-AP). The same antibodies are applied to both C2C12 cells and Drosophila for Western blot.

Transmission Electron Microscopy

For electron microscopy (EM) study on C2C12 cells, cells were rinsed with PBS and then fixed in 2.5% glutaraldehyde overnight at 4°C. EM samples were prepared following protocols as described previously [20, 24]. They were sectioned on a Leica EM UC6/FC6 Ultramicrotome. After sections were transferred to copper grids, counter staining was performed with uranyl acetate and lead acetate before EM imaging.

Statistical Analysis

Statistical analysis was performed using the SPSS 24.0 statistical package (Chicago, IL, USA). A parametric test was applied if the data followed normal distribution. Otherwise, non-parametric tests were used. When a correlation between two variables was assessed, Pearson's R correlation coefficient was calculated. When two groups were compared, parametric t or non-parametric Mann–Whitney tests were used. When more than two groups were compared, parametric ANOVA with indicated post hoc tests or non-parametric Kruskal–Wallis were used. Bar graphed data represent mean $\pm$ SD. Significance is indicated by asterisks: N.S. $P>0.05$, $*P< 0.05$, $**P< 0.01$, $***P< 0.001$, $****P < 0.0001$. Actual p-values of each test are indicated in the corresponding figure legend.

Result

Clinical Features of ALS Patients

In this study, we recruited a cohort of 41 unrelated ALS patients (Patient 1 to 41). An overview of patient clinical data is shown in Table 1. The average age of onset was 39.95 ± 11.37 years. The median time from onset to diagnosis was 6 years (5–15). Seven (6 males and 1 female) of 41 came from 7 independent ALS families, most of them had limb weakness as their first symptom. Eighteen (11 males and 7 females) of 41 were sporadic ALS cases, in whom 14 experienced weakness of extremities, 3 developed dysphagia or dysarthria initially, and 1 had spinal cord symptoms. The other 16 ALS patients had no detailed clinical data.

Nine patients carrying a SOD1 variant suffered from ALS at the ages of 42, 41, 68, 44, 53, 43, 45, 51, and 38 years. Four of them were FALS patients, and seven out of nine patients developed motor symptoms in the lower limbs. Conversely, seven patients carrying a *FUS* mutation (2 females and 5 males) developed their first symptoms at the ages of 15, 24, 28, 42, 21, 32, and 19 years. Patient two had a bulbar onset, patient seven developed spinal cord disease, and the others had limb weakness. The onset age of ALS patients with *FUS* mutation was 25.85 ± 9.08, while the onset age of ALS patients with *SOD1* mutation was 46.33 ± 8.54. The onset ages of the patients with *FUS* mutant were significantly younger than those with *SOD1* mutant. More importantly, an increase in creatine kinase was found in patient one, three, and four with a *FUS* mutation, suggesting the presence of an underlying myogenic lesion.

Lipid Droplet Accumulation in the Skeletal Muscles of ALS Patients

In our previous study, the main pathological feature of skeletal muscle in ALS patients with a *FUS* mutation was found to be neurogenic skeletal muscle damage accompanied by an accumulation of lipid droplets, mainly involving type I muscle fibers [7]. To further explore whether ALS patients are more prone to having abnormal lipid metabolism compared to normal subjects, we compared the degree of lipid droplet accumulation in skeletal muscles between ALS patients (*n*=41) and non-ALS control subjects (*n*=53), as well as different genotypes of ALS.

In ALS patients with *FUS* mutations, muscle tissue ORO staining showed a significant increase in the amount of lipid droplets found in muscle fibers, mainly type I fibers (Fig. 1A–C), which supported the possibility that a disorder of lipid metabolism was occurring. Similarly, ORO staining of muscle tissue showed a significant increase in lipid droplets within muscle fibers of ALS patients with *GRN*, *SOD1*, or *TARDBP* mutations compared to the control group (Fig. 1D–F), although slight lipid droplet accumulation was also found in type I fibers from non-ALS control subjects (Fig. 1G–I). Even so, quantitative analysis found that the degree of lipid droplet accumulation in the muscle tissue of ALS patients was significantly higher than that of the control group (Fig. 1J). In addition, the number of lipid droplets accumulated in the muscle fibers of patients from the *FUS* mutant group was significantly higher than that of patients from either the control group or the other ALS genotype groups (Fig. 1K). At the same time, we found that the lipid droplet ratio associated with the K510Q mutation was not significantly different from other *FUS* mutations (Fig. 1L).

Table 1 Clinical and genetic data on 41 ALS patients

| Patient	Gender	Age	Age of onset(y)	Disease duration(m)	Location of onset	ck(u/l)	Family history	Genetic mutant
1	F	16	15	6	RUE	832	SALS	FUS, p.P525L
2	F	25	24	5	Bulbar	120	SALS	FUS, p.R495*
3	M	29	28	6	RUE	1559	SALS	FUS, p.K510Q
4	M	42	42	4	LLE	2959	FALS	FUS, p.R521H
5	M	22	21	8	LUE	NA	FALS	FUS, p.K510Q
6	M	19	32	24	LUE	NA	SALS	FUS, p.P525L
7	M	34	19	3	Spinal	NA	SALS	FUS, p.P525L
8	F	42	41	6	LUE	138	SALS	SOD1, p.G42S
9	F	41	40	6	RLE	NA	SALS	SOD1, p.G142E
10	M	53	52	5	RLE	560	SALS	NI
11	M	68	65	6	RLE	484	SALS	SOD1, p.G62A
12	M	44	44	3	LLE	NA	SALS	SOD1, p.A146T
13	M	53	53	2	LLE	100	FALS	SOD1, p.G142A
14	M	43	43	3	RLE	NA	FALS	SOD1, p.G142A
15	F	45	44	12	LUE	NA	FALS	SOD1, p.G42D
16	F	51	50	6	RUE	100	NA	SOD1, p.S69S
17	M	38	37	6	LLE	473	FALS	SOD1, p.G42D
18	M	62	60	24	LUE	266	FALS	NI
19	M	41	39	24	LLE	NA	NA	NI
20	F	36	34	18	Bulbar	NA	SALS	NI
21	F	52	51	8	RLE	NA	NA	NI
22	M	40	39	12	RLE	NA	SALS	NI
23	M	32	31	6	RUE	353	SALS	NI
24	F	38	37	6	RLE	NA	NA	NI
25	F	42	41	12	LUE	55	NA	NI
26	M	49	48	6	LLE	337	NA	GRN, p.R538Q
27	F	30	28	24	RUE	NA	NA	NI
28	M	55	53	24	LLE	NA	NA	MATR3, p.N787S
29	M	48	47	12	LLE	NA	NA	NI
30	M	46	46	2	RLE	NA	SALS	NEFH, p.S787R
31	M	47	46	8	RUE	NA	SALS	NI
32	F	44	44	4	LUE	NA	NA	GRN, p.T18K
33	F	50	48	24	LLE	NA	NA	NI
34	M	47	46	8	RUE	NA	SALS	TBK1, p.I334T
35	M	24	24	4	RUE	NA	NA	VCP, p.R89Q
36	F	29	26	30	RUE	NA	SALS	NIPA1, p.A13V
37	F	51	49	24	RUE	245	NA	NI
38	M	36	31	60	RUE	828	NA	NI
39	F	33	33	1	Bulbar	NA	SALS	TARDBP, p.N378D
40	F	50	49	6	LUE	265	NA	BICD2, p.N731S
41	F	38	37	12	LUE	NA	NA	NI

F: female; *M*: male; *SALS*: sporadic amyotrophic lateral sclerosis; *FALS*: family amyotrophic lateral sclerosis; *NA*: not available; *RUE*: right upper limb; *LUE*: left upper limb; *RLE*: right lower limb; *LLE*: left lower limb; *NI*: not identified

Establishment and Characterization of the C2C12 Cell Model with FUS-K510Q Mutation

Our previous work has demonstrated that K510Q and P525L mutations show similar pathological features in cells [12, 16, 20]. Since all ALS patients with *FUS* mutations showed similar lipid droplet accumulation in skeletal muscle, we established a cellular model in which a myoblast cell line (C2C12) was modified using adenovirus transduction to overexpress mutant FUS (FUS-K510Q) to investigate whether mutant FUS expression leads to disordered lipid metabolism in muscle cells. FUS protein expression was examined at 24-h, 48-h, or 72-h post-transduction. The results showed that the expression

Fig. 1 Lipid droplet accumulation in the skeletal muscle of ALS patients. **A–I** Oil Red O staining of skeletal muscle sections (scale bar: 100μm). **A–C** ALS patients with *FUS* mutations. **D–F** ALS patients with GRN, SOD1, and TAR-DBP gene mutation, respectively. **G–I** Non-ALS control subjects. **J** Lipid droplet ratio was determined and compared between Ctr (*n*=53) and ALS (*n*=41) (****$p<0.0001$). **K** Lipid droplet ratio of different genotypes of ALS and control were determined, NI: unidentified variants, Other: other pathogenic gene mutations, Ctr: Non-ALS control subjects (***$p<0.001$, ****$p<0.0001$). **L** The lipid droplet ratio of ALS patients with different FUS gene mutation loci was determined. *: Stop codon (N.S.: *p>0.05*)
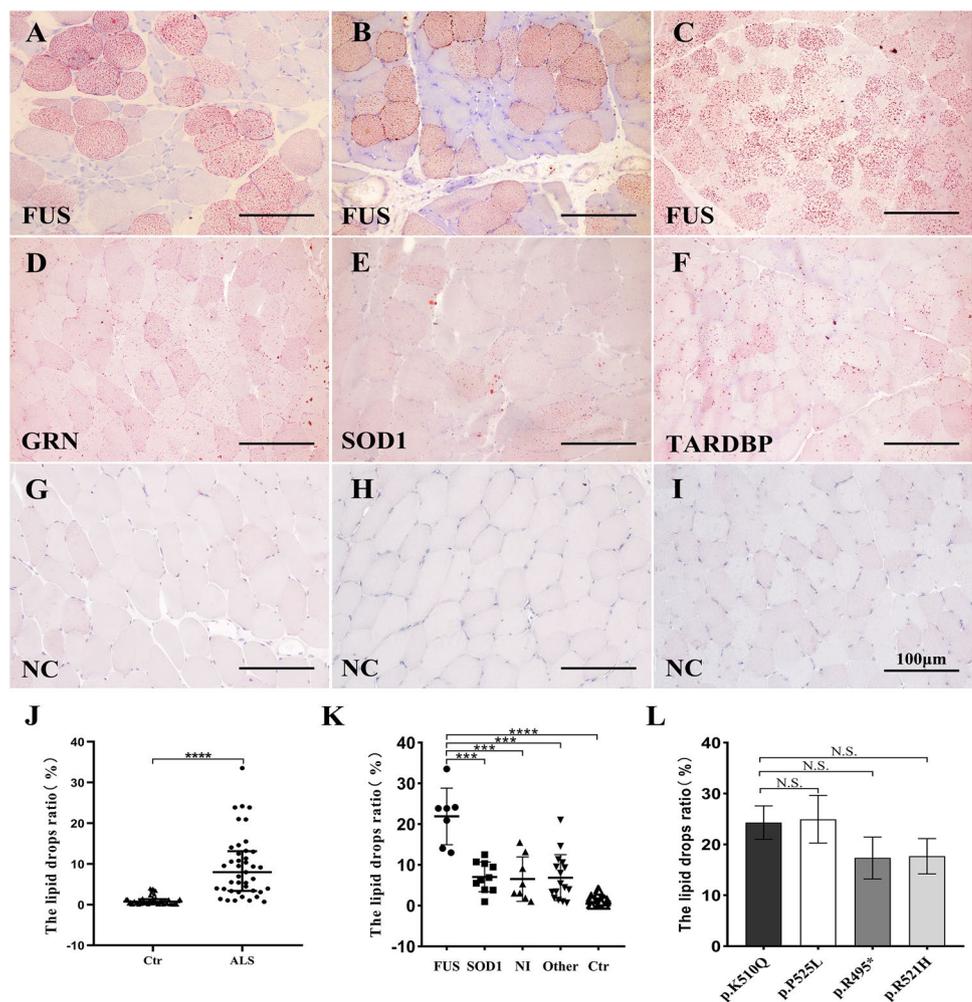
level of FUS protein in the FUS-K510Q mutant group was significantly higher than that in the control group at 24-h post-transduction, and FUS protein expression peaked at 48 h (Fig. 2A, B). It should be noted that after FUS protein expression reached its peak at 48 h, we were ready to induce muscle cell differentiation, but the muscle cells significantly died at 72-h post-transduction, so we were unable to establish a differentiated C2C12 myotube model expressing the FUS-K510Q mutant. Thus, we selected the 48-h transduction time point for subsequent experiments.

Next, we performed immunofluorescence staining of FUS protein in C2C12 cells expressing FUS-K510Q. As shown in Fig. 2C, FUS proteins were mainly distributed in the nucleus in the Ctr group. In contrast, C2C12 cells expressing FUS-K510Q showed abnormal cytoplasmic localization of FUS proteins, and FUS missing a nuclear localization. This indicates nuclear clearance of endogenous wild-type FUS protein in myoblasts expressing FUS-K510Q, which mimic the main pathological feature of ALS.

Expression of FUS-K510Q Mutant Causes Muscle Cell Death and Disordered Lipid Metabolism

To investigate the cytotoxicity of mutant FUS in myoblasts, cells expressing Ctr, Wt or K510Q mutant FUS were evaluated cell viability at 48 h. Consistent with the previous studies [12, 20], it showed that the viability of cells expressed Wt or K510Q mutant FUS was significantly decreased compared with the Ctr, meanwhile the cells expressing K510Q mutant showed higher cytotoxicity compared with Wt (Fig. S1). To examine the relationship between FUS mutation and lipid metabolism in myoblasts, C2C12 cells expressed Ctr, Wt, or ALS-associated K510Q mutant FUS for 48 h and were then subjected for Oil Red O staining. The results showed that intracellular lipid droplet deposition was increased in the FUS-K510Q group compared to the Ctr and Wt groups before or after 0.25 mM oleic acid treatment (Supplementary Fig. 3A, S2A and S3A), and further quantitative analysis showed that the intracellular lipid droplet ratio was significantly elevated in the FUS-K510Q group compared to the Ctr and Wt groups

Fig. 2 C2C12 cell line expressing FUS-K510Q. **A**, **B** Analysis of FUS protein levels by western blotting at different time points after Ctr (empty vector) or FUS-K510Q expression in C2C12 cells; β-Actin was used as an internal control (**$p<0.01$). **C** Confocal images of C2C12 cells expressing Ctr (empty vector) or FUS-K510Q (scale bar: 25μm)
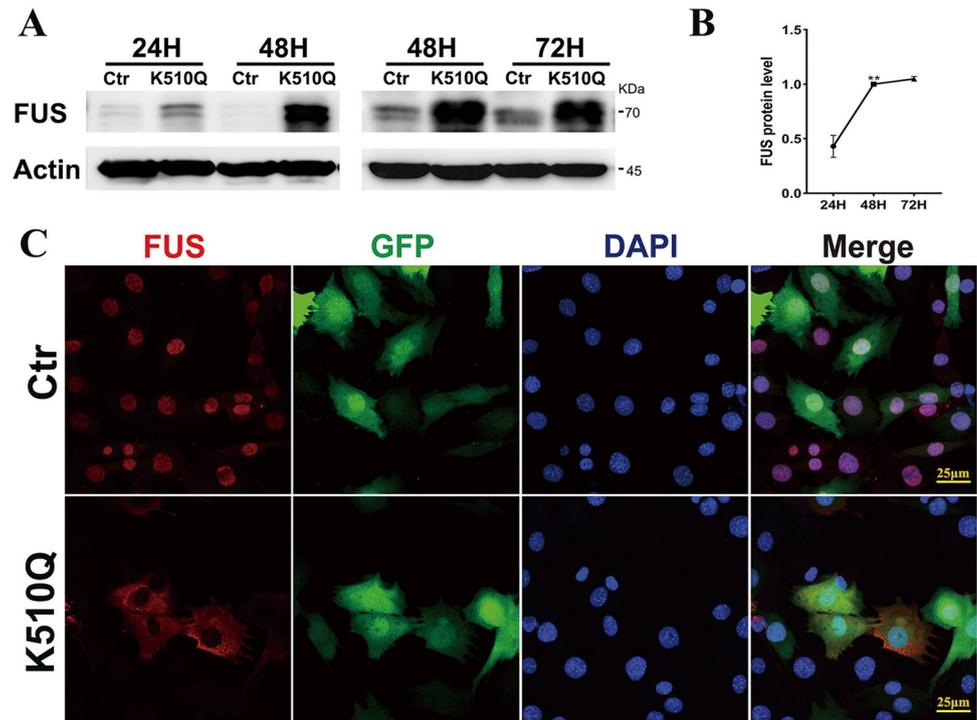
(Supplementary Fig. 3B, S2B and S3B). It should be noted that the lipid storage in myoblasts expressing Wt FUS had no significant increase compared with Ctr, although it exhibited cytotoxicity. Thus, we investigated the disordered lipid metabolism in ALS using cells expressing Ctr and FUS-K510Q mutant in subsequent experiments.

To further study the morphology and distribution of lipid droplets in cells, EM analysis was performed on cells expressing Ctr and FUS-K510Q. After 0.25 mM OA treatment, normal nuclei and mitochondrial structures could be observed in the cells expressing Ctr, with only a few areas of lipid droplet deposition. In contrast, cells expressing FUS-K510Q were found to have an increased number of lipid droplets deposited in the vicinity of mitochondria (Fig. 3C).

Expression of FUS-K510Q Mutant Causes Mitochondrial Dysfunction

To investigate whether expression of the FUS mutant leads to mitochondrial dysfunction in myoblasts, we measured intracellular ROS levels by using the fluorescent probe DHE. The results showed that the fluorescence intensity of intracellular ROS in C2C12 cells expressing the FUS-K510Q mutation was significantly higher than that of Ctr-expressing C2C12 cells (Fig. 4A, B). In addition, we detected mitochondrial membrane potential levels by using TMRM to stain live cell. Compared with Ctr-expressing cells, the fluorescence intensity of TMRM in myoblasts expressing the FUS-K510Q mutation was significantly decreased (Fig. 4C, D). We further explored whether overexpression of FUS-K510Q would lead to insufficient ATP production, and we found that ATP level of myoblasts expressing FUS-K510Q mutation was significantly decreased compared to Ctr-expressing cells (Fig. 4E). In addition, EM study showed that the morphology of the nucleus, endoplasmic reticulum, and mitochondria were normal in the Ctr group, while the FUS-K510Q mutant group presented with aggregated mitochondria, abnormal mitochondria (indicated by thick white arrows), and deposition of lipid droplets in the cytoplasm (indicated by thin white arrows) (Fig. 4F). These results indicate that overexpression of the FUS-K510Q mutation in C2C12 cells leads to mitochondrial dysfunction, accompanied by disordered lipid metabolism.

FUS-K510Q Mutant Alters the Expression Level of Lipid Metabolism-Related Genes

To further explore the molecular mechanism by which FUS-K510Q impairs lipid metabolism, several proteins related to fatty acid metabolism were examined, including carnitine palmitoyl transferase 1A (CPT1A), adipose triglyceride lipase (ATGL), and adipose differentiation-related protein

Fig. 3 Expression of FUS-K510Q causes disordered lipid metabolism. **A** Oil Red O staining of C2C12 cells under 0.25 mM OA treatment. **B** The lipid droplet ratio was measured and quantified using Image-Pro Plus software (**$p<0.01$). **C** Electron microscopic images of C2C12 cells expressing Ctr (empty vector) or FUS-K510Q for 48 h and under 0.25 mM OA treatment, thick white arrows: lipid droplets
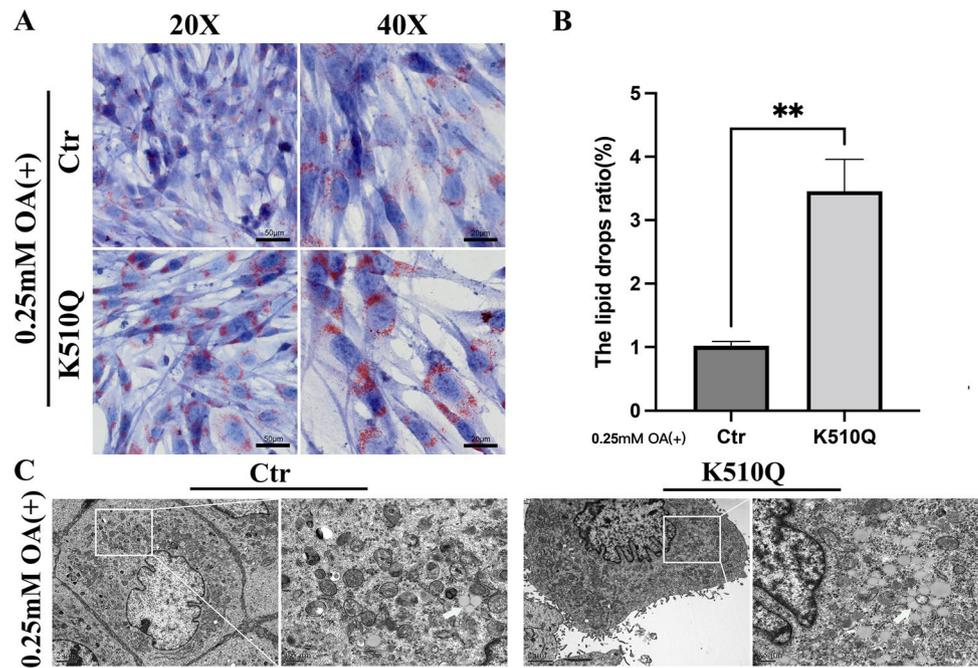
(PLIN2). As shown in Fig. 5A, compared with Ctr-expressing cells, PLIN2 expression was significantly upregulated in cells expressing FUS-K510Q, while the ATGL expression was downregulated. At the same time, although CPT1A expression was not statistically altered, a downwards trend could be observed (Fig. 5A, C–F). We also detected protein levels after 0.25 mM OA treatment. Consistently, we found that compared with Ctr-expressing cells, PLIN2 expression was significantly upregulated in cells expressing FUS-K510Q, while the levels of ATGL and CPT1A were downregulated (Fig. 5B–F).

FUS-K510Q-Expressing Flies Show Locomotor Defects and Dysregulated Lipid Metabolism

To investigate the intrinsic toxicity or cell-autonomous toxicity in ALS muscle cells, and the molecular mechanism driving disordered lipid metabolism, FUS-K510Q mutant protein was expressed specifically in the thoracic flight muscles of Drosophila under a Mef2-Gal4 driver. It should be noted that the F1 flies with a genetic background of Mef2-Gal4/UAS-FUS-K510Q were lethal and could not survive to the pupa stage. This indicates that the mutant FUS protein is toxic in muscle cells in vivo. Then, we used a system in which FUS-K510Q expression was induced only in adulthood using a temperature-sensitive Tub-Gal80^{ts} promoter with a Mef2-Gal4 muscle-specific driver. In this system, flies expressing FUS-K510Q in muscle following heat shock induction in adulthood indeed exhibited significant locomotor defects at 35 days old compared with Ctr-expressing flies (Fig. 6A, B, supplemental video 1).

To confirm whether expression of FUS-K510Q mutant dysregulated lipid metabolism in vivo, triglyceride levels were examined in the flight muscles of flies expressing Ctr or FUS-K510Q. The results revealed that triglyceride levels were significantly higher in the FUS-K510Q mutation group compared to the Ctr group (Fig. 6C). Consistent with the findings in myoblasts, PLIN2 expression was significantly upregulated in fly muscle expressing FUS-K510Q compared to the Ctr, while ATGL and CPT1A protein levels were downregulated significantly (Fig. 6D–H). These results indicate that FUS mutation causes toxicity in muscle cells, and disordered lipid metabolism may be one of the mechanisms driving ALS disease pathology.

Discussion

Muscle atrophy and weakness associated with ALS has long been attributed to motor neuron loss alone, however several studies in ALS patients and ALS animal models have challenged this assumption by providing direct evidence that muscle can play an active role in disease [25–27]. Recent studies on the skeletal muscle of ALS patients found that phosphorylated TAR DNA-binding protein 43 (pTDP-43) aggregates appeared in the muscle fibers and autophagy-related gene SQSTM1 expression level was up-regulated significantly, indicating that skeletal muscle could be an additional pathological target of pTDP-43 [25]. In addition, studies on animal models found that: (1) overexpressing UCP1 in mice as a way to produce muscle-specific mitochondrial uncoupling resulted in progressive deterioration

Fig. 4 Expression of FUS-K510Q causes mitochondrial dysfunction. **A**, **B** Intracellular ROS level was detected in cells expressing Ctr (empty vector) or FUS-K510Q for 48 h by using DHE staining and images were captured by inverted fluorescence microscopy (scale bar: 25μm), GFP: green; DHE: red; DAPI: blue. ROS levels were measured and quantified in a bar graph (*n*>100, ****: *p*<0.0001). **C**, **D** Mitochondrial membrane potential was detected in cells expressing Ctr (empty vector) or FUS-K510Q for 48 h by using TMRM staining and images were captured by inverted fluorescence microscopy (scale bar: 25μm), GFP: green; TMRM: red; DAPI: blue. The membrane potential was measured and quantified in a bar graph (n>100, ****: *p*<0.0001). **E** Intracellular ATP levels in cells expressing Ctr (empty vector) or FUS-K510Q for 48h were detected; data represents four independent experiments and was analyzed using two-tailed *t*-test (***: *p*<0.001). **F** Electron microscopic images of C2C12 cells expressing Ctr (empty vector) or FUS-K510Q for 48 h, thick white arrows: mitochondria; thin white arrows: lipid droplets
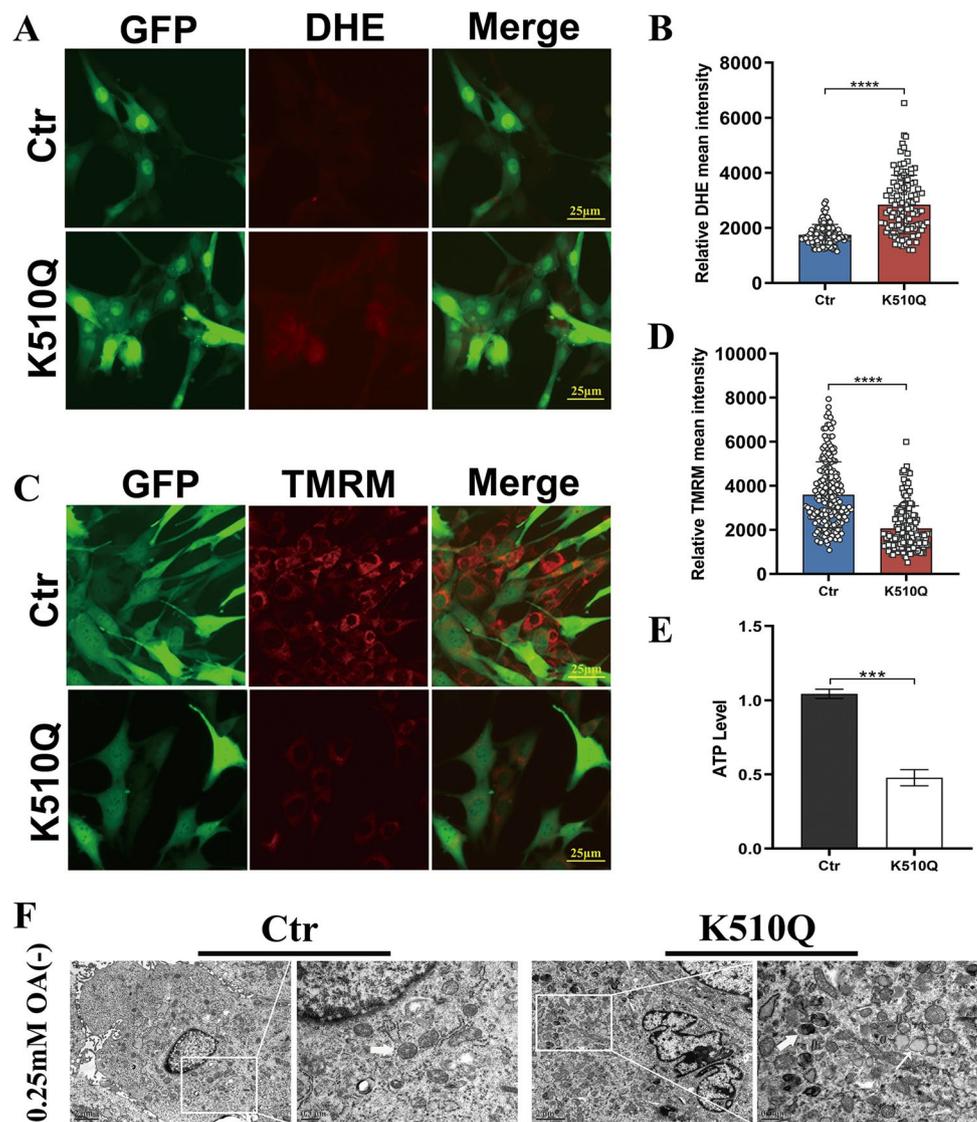
of the neuromuscular junction followed by denervation and mild late-onset motor neuron pathology [26]; (2) overexpressing SOD1 mutant protein in mouse muscle showed ALS pathological features, including muscle degeneration, abnormal neuromuscular junction, and motor neuron degeneration, suggesting a muscle-to-motor neuron "dying-back" phenomenon [27]. In this study, we also found that primary pathogenic changes to muscle cells might be involved in the pathogenesis of ALS.

Muscle degeneration in ALS-related disorders can be associated with an imbalance between protein synthesis and degradation in the muscle, or abnormal changes in energy metabolism. Britto Caves-Filho et al. found mitochondrial abnormalities in motor neurons and lipid droplet accumulation in abnormal astrocytes by lipidomic analysis in motor cortex and spinal cord tissues from SOD1-G93A and WT rats during asymptomatic period (~70 days) and symptomatic period (~120 days) [10], but the mechanism of lipid metabolism in ALS-affected muscles has not been elucidated. Studies have shown that increased amounts of glycolytic enzyme G3PDH were found by mass spectrometry in mouse models of motor neuron disease, indicating a shift from oxidative metabolism to glycolysis during disease progression [28]. Scaricamaza et al. found that metabolic reprogramming of skeletal muscle preceded disease onset in ALS-SOD1 G93A mice [11]. In addition, Chiang et al. found that deletion of TDP-43 down-regulated the obesity-related gene Tbc1d1 and altered body fat metabolism by constructing TDP-43 KO mice [29]. Collectively, previous studies have revealed that the metabolic dysfunction, especially the lipid metabolism, might be closely associated with the ALS pathogenesis. In this study, we found that a large number of muscle fibers in ALS patients showed a moderate to severe increase in lipid droplet accumulation.

Fig. 5 Expression of FUS-K510Q alters expression of CPT1A, ATGL, and PLIN2. **A** Western blot analysis of FUS, ATGL, CPT1A, and PLIN2 at the protein level in cells expressing Ctr (empty vector) or FUS-K510Q for 48h; β-Actin was used as an internal control. **B** Under 0.25 mM OA treatment, western blot analysis of FUS, ATGL, CPT1A, and PLIN2 protein levels in cells expressing Ctr or FUS-K510Q for 48h. **C–F** Quantification of FUS, ATGL, CPT1A, and PLIN2 protein levels in respective groups. Data are presented as the means ± SD. Data were collected from three independent experiments and analyzed using two-tailed t-test (N.S.: $p>0.05$, *$p<0.05$, **$p<0.01$, ****$p<0.0001$)
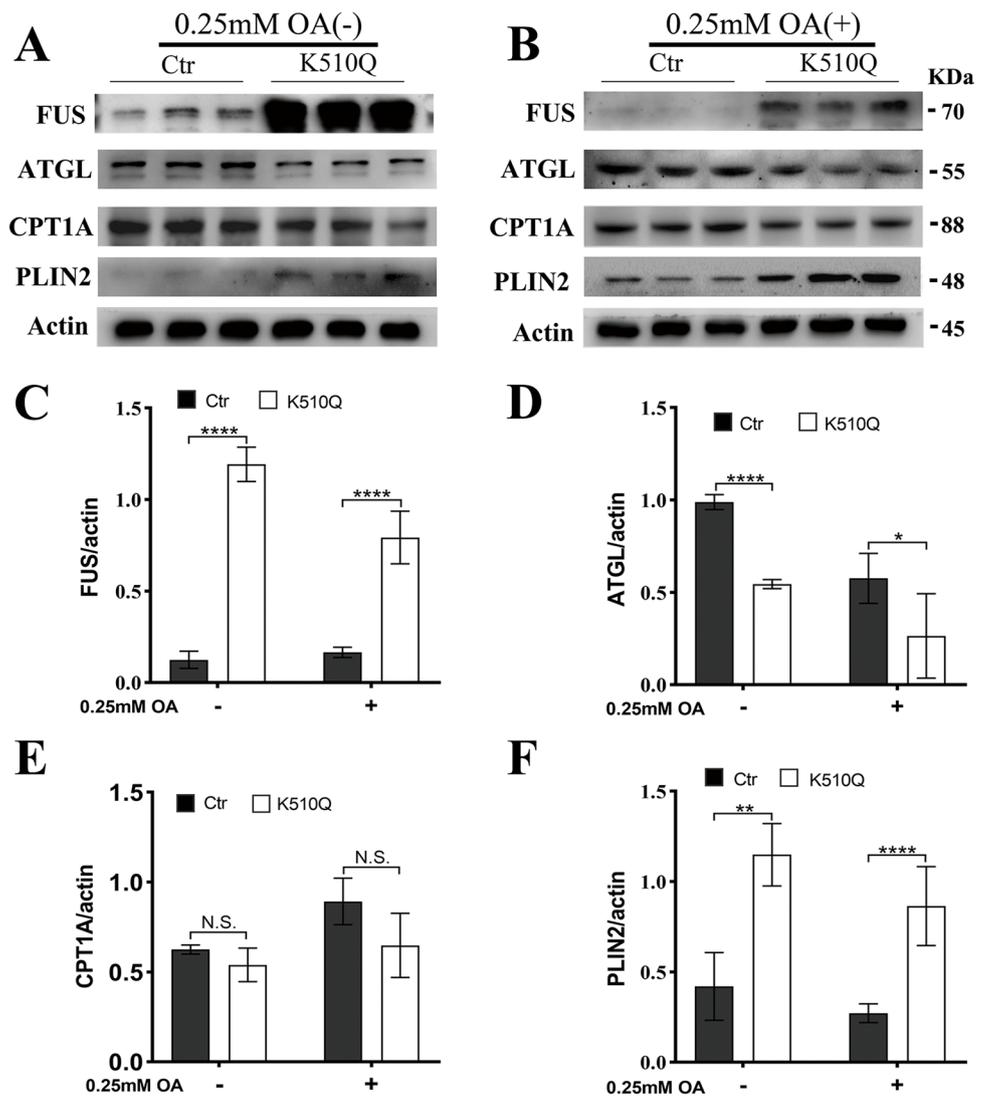
Among different genotypes, ALS patients with *FUS* mutations were more likely to have lipid droplets accumulating than other ALS patients with different gene mutations. To further investigate the relationship between *FUS* mutations and lipid metabolism in myocytes, we established a muscle-specific FUS-K510Q mutant cell model and a *Drosophila* model. Both *in vitro* and *in vivo* studies showed FUS-K510Q increased lipid droplet accumulation in myocytes. Moreover, we used Mef2-Gal4 to specifically express the FUS mutant protein in fly muscle and examined locomotive ability. The results showed that flies expressing the FUS mutant protein had locomotor deficits, mimicking the ALS phenotype, and further suggested the possibility of intramuscular toxicity. Studies have shown that oral creatine supplementation as an energy source is beneficial for SOD1 mutant mice [30]. Similarly, in SOD1 mutant mice, L-carnitine-stimulated beta-oxidation of fatty acids improves motor function and prolongs survival [31]. Here,

we provide evidence that muscle metabolic dysfunctions occur in ALS, suggesting that skeletal muscle may be an important target for the treatment of this disease.

Mitochondria play an important role in energy production, metabolism, intracellular signaling [32, 33], free radical generation [34, 35], autophagy [36, 37], and other pathways [38], and mitochondrial dysfunction is highly relevant to the onset of neurodegenerative diseases. There is an increasing amount of evidence showing that FUS and TDP-43 are closely associated with mitochondrial dysfunction [39]. FUS and TDP-43 not only localize to mitochondria, but also regulate mitochondrial biological functions. It has been reported that oxidative damage caused by an increase in reactive oxygen species leads to mitochondrial dysfunction, which is also known to contribute to ALS pathogenesis [40]. Studies have shown that inhibitors of mitochondrial OXPHOS can induce triglyceride accumulation in pre-adipocytes and maintain a fibroblast phenotype, and pre-adipocytes cannot differentiate into adipocytes and
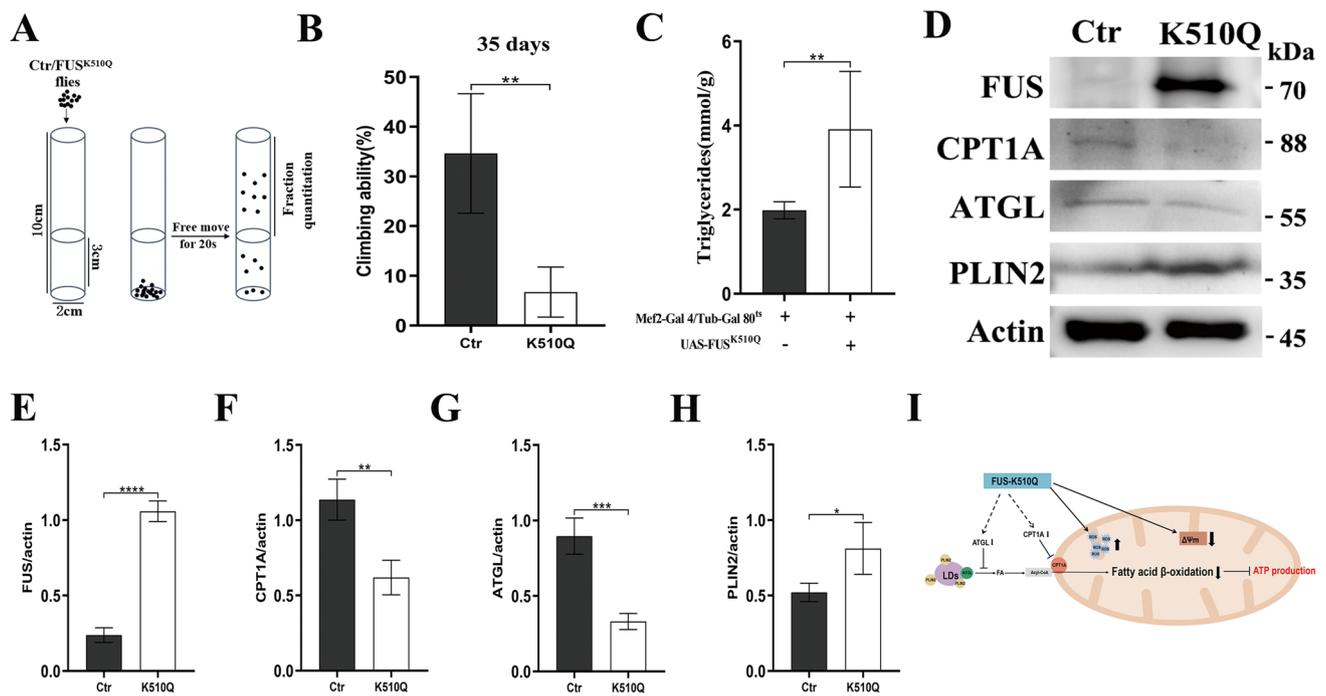
Fig. 6 Expression of FUS-K510Q in fly muscle leads to locomotor defects and dysregulated lipid metabolism. **A** Model diagram of climbing assay used to assess climbing ability in adult flies. **B** Climbing ability was measured in adult flies at 35 days old following induction of Ctr or FUS-K510Q mutant expression under the Mef2-Gal4/Tub-Gal80^{ts} driver. Expression of FUS-K510Q in fly muscles led to severe locomotor deficits. More than 100 flies were measured in each group (repeat 6 times per group, **$p < 0.01$). **C** Triglycerides levels in fly muscles were detected and quantified ($n = 3$, **$p < 0.01$). **D–H** Representative western blot and quantitative analysis of FUS, ATGL, CPT1A, and PLIN2 protein level in the flight muscles of flies; β-Actin was used as an internal control. Data are presented as the means ± SD. Data were collected from three independent experiments and analyzed using two-tailed t-test (*$p < 0.05$, **$p < 0.01$, ***$p < 0.001$, ****$p < 0.0001$). **I** Working model diagram of the mutant FUS-K510Q protein causing disordered lipid metabolism and mitochondrial dysfunction. Fly genotypes: Ctr: Mef2-Gal4/Tub-Gal80^{ts}/W1118; FUS-K510Q: Mef2-Gal4/Tub-Gal80^{ts}/UAS-K510Q-FUS

acquire adipogenic markers [41]. In muscle cells, fatty acids accumulate near mitochondria and these fatty acids are susceptible to reactive oxygen species (ROS)-induced oxidative damage, leading to the formation of lipid peroxides, which in turn leads to oxidative damage to the mitochondrial machinery [42]. Our previous studies indicated that mutant FUS protein interacts with HSP60 to localize into mitochondria and mutant FUS protein disrupts the assembly of ATP synthase complexes by directly interacting with ATP5B [12, 20]. Here, we found that in myoblasts expressing FUS mutant proteins, ROS levels were significantly upregulated, membrane potential levels were downregulated, and ATP production was reduced, which are all consistent with the findings from our previous studies [12, 16]. These results suggest that FUS mutations may be closely related to mitochondrial dysfunction in muscle cells, although it is uncertain whether mitochondrial dysfunction precedes, is independent of, or is the consequence of lipid alterations. In previous studies, both Wt and mutant FUS caused mitochondrial dysfunction and cytotoxicity [12, 20]. Consistently, we found Wt FUS induced cytotoxicity in myoblasts, but not lipid droplet accumulation. It is likely that lipid droplet accumulation is independent of mitochondrial dysfunction in cells expressing Wt FUS. Future studies are required to elucidate the relationship between lipid droplet accumulation and mitochondrial dysfunction in cellular or animal models expressing mutant FUS.

Lipid droplets are neutral lipid storage organelles that play an important role in energy homeostasis and lipid metabolism through their interactions with mitochondria [43]. Generally, the fatty acids taken up by muscle cells will eventually be converted into triglycerides and stored in lipid droplets. Under physiological conditions, the breakdown of lipid droplets is mainly mediated by triglyceride hydrolases and diglyceride hormone-sensitive lipases in the lipolysis pathway, and then the glycerol and fatty acids produced by the hydrolysis of lipid are transported to the inner mitochondrial membrane for beta-oxidation of fatty acids, and finally ATP is generated. Through the muscle-specific cell model and *Drosophila* model, we found that the PLIN2 protein level was significantly upregulated compared with Ctr-expressing groups, while the ATGL and CPT1A protein levels were significantly downregulated in FUS mutant groups. These results suggest that *FUS* mutations may inhibit lipolysis and mitochondrial transport of acyl-CoA (Fig. 6I).

There are still some limitations to our study. Firstly, we only observed the accumulation of lipid droplets in cells expressing K510Q mutant FUS, although K510Q, R512L, and P525L mutant FUS were all found to cause lipid droplet accumulation in the skeletal muscle of ALS patients. Since muscle cells expressing FUS-K510Q begin to die at 72-h post-transduction, we have not been able to detect any functional changes occurring in C2C12 cells after they differentiate into myotubes. Secondly, although Mef2-Gal4 expressed FUS-K510Q strongly in fly muscles, it may also have leakage expression in a few neurons that contribute to the motor defects observed in our drosophila model. Further studies on iPSC-derived muscle cells are needed to support the hypothesis of FUS-induced intramuscular toxicity.

In summary, our study uncovered the possible relationship between mitochondrial dysfunction and disordered lipid metabolism in ALS-FUS skeletal muscle. The data presented in this study led us to propose the following working model: Firstly, the FUS-K510Q mutant protein causes mitochondrial dysfunction, including loss of membrane potential and increased ROS production in myocytes. Secondly, FUS-K510Q mutant protein downregulates ATGL protein levels, leading to reduced lipolysis, thereby increase the accumulation of cytoplasmic lipid droplets. Altogether, mitochondrial dysfunction and impaired lipolysis eventually inhibit fatty acid β-oxidation, leading to decreased ATP production (see working model in Fig. 6I).

Declarations

Ethics Approval The protocol was approved by the Ethics Committee of the First Affiliated Hospital of Nanchang University and the First Hospital of Peking University. All patients obtained informed consent to participate in the study.

Consent to Participate Not applicable.

Consent for Publication Not applicable.

Conflict of Interests The authors declare no competing interests.

References

1. Statland JM, Barohn RJ, McVey AL, Katz JS, Dimachkie MM (2015) Patterns of weakness, classification of motor neuron disease, and clinical diagnosis of sporadic amyotrophic lateral sclerosis. Neurol Clin 33(4):735–748. https://doi.org/10.1016/j.ncl.2015.07.006
2. Chia R, Chiò A, Traynor BJ (2018) Novel genes associated with amyotrophic lateral sclerosis: diagnostic and clinical implications. Lancet Neurol 17(1). https://doi.org/10.1016/S1474-4422(17)30401-5
3. Kiernan MC, Vucic S, Cheah BC, Turner MR, Eisen A, Hardiman O, Burrell JR, Zoing MC (2011) Amyotrophic lateral sclerosis. Lancet 377(9769):942–955. https://doi.org/10.1016/S0140-6736(10)61156-7
4. Menon P, Kiernan MC, Vucic S (2014) ALS pathophysiology: insights from the split-hand phenomenon. Clin Neurophysiol 125(1):186–193. https://doi.org/10.1016/j.clinph.2013.07.022
5. Dupuis L, Echaniz-Laguna A (2010) Skeletal muscle in motor neuron diseases: therapeutic target and delivery route for potential treatments. Curr Drug Targets 11(10):1250–1261. https://doi.org/10.2174/1389450111007011250
6. Picchiarelli G, Demestre M, Zuko A, Been M, Higelin J, Dieterlé S, Goy M-A, Mallik M et al (2019) FUS-mediated regulation of acetylcholine receptor transcription at neuromuscular junctions is compromised in amyotrophic lateral sclerosis. Nat Neurosci 22(11):1793–1805. https://doi.org/10.1038/s41593-019-0498-9
7. Zhou B, Wang H, Cai Y, Wen H, Wang L, Zhu M, Chen Y, Yu Y et al (2020) FUS P525L mutation causing amyotrophic lateral sclerosis and movement disorders. Brain Behav 10(6):e01625. https://doi.org/10.1002/brb3.1625
8. Farese RV, Walther TC (2009) Lipid droplets finally get a little R-E-S-P-E-C-T. Cell 139(5):855–860. https://doi.org/10.1016/j.cell.2009.11.005
9. Angelini C, Nascimbeni AC, Cenacchi G, Tasca E (2016) Lipolysis and lipophagy in lipid storage myopathies. Biochim Biophys Acta 1862(7):1367–1373. https://doi.org/10.1016/j.bbadis.2016.04.008
10. Chaves-Filho AB, Pinto IFD, Dantas LS, Xavier AM, Inague A, Faria RL, Medeiros MHG, Glezer I et al (2019) Alterations in lipid metabolism of spinal cord linked to amyotrophic lateral sclerosis. Sci Rep 9(1):11642. https://doi.org/10.1038/s41598-019-48059-7
11. Scaricamazza S, Salvatori I, Giacovazzo G, Loeffler JP, Renè F, Rosina M, Quessada C, Proietti D et al (2020) Skeletal-muscle metabolic reprogramming in ALS-SOD1 mice predates disease onset and is a promising therapeutic target. iScience 23(5):101087. https://doi.org/10.1016/j.isci.2020.101087
12. Deng J, Wang P, Chen X, Cheng H, Liu J, Fushimi K, Zhu L, Wu JY (2018) FUS interacts with ATP synthase beta subunit and induces mitochondrial unfolded protein response in cellular and animal models. Proc Natl Acad Sci U S A 115(41):E9678–E9686. https://doi.org/10.1073/pnas.1806655115
13. Bollinger LM, Campbell MS, Brault JJ (2018) Palmitate and oleate co-treatment increases myocellular protein content via impaired protein degradation. Nutrition 46:41–43. https://doi.org/10.1016/j.nut.2017.07.017

14. Capel F, Cheraiti N, Acquaviva C, Hénique C, Bertrand-Michel J, Vianey-Saban C, Prip-Buus C, Morio B (2016) Oleate dose-dependently regulates palmitate metabolism and insulin signaling in C2C12 myotubes. Biochim Biophys Acta 1861(12 Pt A):2000–2010. https://doi.org/10.1016/j.bbalip.2016.10.002

15. Liu X, Chen J, Li X, Gao S, Deng M (2014) Generation of induced pluripotent stem cells from amyotrophic lateral sclerosis patientcarrying SOD1-V14M mutation. Zhonghua Yi Xue Za Zhi 94(27):2143–2147

16. Deng J, Wu W, Xie Z, Gang Q, Yu M, Liu J, Wang Q, Lv H et al (2019) Novel and recurrent mutations in a cohort of chinese patients with young-onset amyotrophic lateral sclerosis. Front Neurosci 13:1289. https://doi.org/10.3389/fnins.2019.01289

17. Demontis F, Perrimon N (2010) FOXO/4E-BP signaling in Drosophila muscles regulates organism-wide proteostasis during aging. Cell 143(5):813–825. https://doi.org/10.1016/j.cell.2010.10.007

18. McGuire SE, Mao Z, Davis RL (2004) Spatiotemporal gene expression targeting with the TARGET and gene-switch systems in Drosophila. Sci STKE 2004(220):l6

19. Ranganayakulu G, Zhao B, Dokidis A, Molkentin JD, Olson EN, Schulz RA (1995) A series of mutations in the D-MEF2 transcription factor reveal multiple functions in larval and adult myogenesis in Drosophila. Dev Biol 171(1):169–181

20. Deng J, Yang M, Chen Y, Chen X, Liu J, Sun S, Cheng H, Li Y et al (2015) FUS interacts with HSP60 to promote mitochondrial damage. PLoS Genet 11(9):e1005357. https://doi.org/10.1371/journal.pgen.1005357

21. Li Y, Ray P, Rao EJ, Shi C, Guo W, Chen X, Woodruff EA, Fushimi K et al (2010) A Drosophila model for TDP-43 proteinopathy. Proc Natl Acad Sci U S A 107(7):3169–3174. https://doi.org/10.1073/pnas.0913602107

22. Viscarra JA, Wang Y, Nguyen HP, Choi YG, Sul HS (2020) Histone demethylase JMJD1C is phosphorylated by mTOR to activate de novo lipogenesis. Nat Commun 11(1):796. https://doi.org/10.1038/s41467-020-14617-1

23. Zhang D, Zhai X, He X-j (2015) Application of oil red O staining in spinal cord injury of rats. Zhongguo Gu Shang 28(8):738–742

24. Deng J, Yu J, Li P, Luan X, Cao L, Zhao J, Yu M, Zhang W et al (2020) Expansion of GGC repeat in GIPC1 is associated with oculopharyngodistal myopathy. Am J Hum Genet 106(6):793–804. https://doi.org/10.1016/j.ajhg.2020.04.011

25. Cykowski MD, Powell SZ, Appel JW, Arumanayagam AS, Rivera AL, Appel SH (2018) Phosphorylated TDP-43 (pTDP-43) aggregates in the axial skeletal muscle of patients with sporadic and familial amyotrophic lateral sclerosis. Acta Neuropathol Commun 6(1):28. https://doi.org/10.1186/s40478-018-0528-y

26. Dupuis L, Gonzalez de Aguilar J-L, Echaniz-Laguna A, Eschbach J, Rene F, Oudart H, Halter B, Huze C et al (2009) Muscle mitochondrial uncoupling dismantles neuromuscular junction and triggers distal degeneration of motor neurons. PLoS One 4(4):e5390. https://doi.org/10.1371/journal.pone.0005390

27. Wong M, Martin LJ (2010) Skeletal muscle-restricted expression of human SOD1 causes motor neuron degeneration in transgenic mice. Hum Mol Genet 19(11):2284–2302. https://doi.org/10.1093/hmg/ddq106

28. Staunton L, Jockusch H, Ohlendieck K (2011) Proteomic analysis of muscle affected by motor neuron degeneration: the wobbler mouse model of amyotrophic lateral sclerosis. Biochem Biophys Res Commun 406(4):595–600. https://doi.org/10.1016/j.bbrc.2011.02.099

29. Chiang P-M, Ling J, Jeong YH, Price DL, Aja SM, Wong PC (2010) Deletion of TDP-43 down-regulates Tbc1d1, a gene linked to obesity, and alters body fat metabolism. Proc Natl Acad Sci U S A 107(37):16320–16324. https://doi.org/10.1073/pnas.1002176107

30. Klivenyi P, Ferrante RJ, Matthews RT, Bogdanov MB, Klein AM, Andreassen OA, Mueller G, Wermer M et al (1999) Neuroprotective effects of creatine in a transgenic animal model of amyotrophic lateral sclerosis. Nat Med 5(3):347–350. https://doi.org/10.1038/6568

31. Kira Y, Nishikawa M, Ochi A, Sato E, Inoue M (2006) L-carnitine suppresses the onset of neuromuscular degeneration and increases the life span of mice with familial amyotrophic lateral sclerosis. Brain Res 1070(1):206–214. https://doi.org/10.1016/j.brainres.2005.11.052

32. Ivanova MI, Sievers SA, Guenther EL, Johnson LM, Winkler DD, Galaleldeen A, Sawaya MR, Hart PJ et al (2014) Aggregation-triggering segments of SOD1 fibril formation support a common pathway for familial and sporadic ALS. Proc Natl Acad Sci U S A 111 (1):197-201. doi:https://doi.org/10.1073/pnas.1320786110

33. Verdin E, Hirschey MD, Finley LWS, Haigis MC (2010) Sirtuin regulation of mitochondria: energy production, apoptosis, and signaling. Trends Biochem Sci 35(12):669–675. https://doi.org/10.1016/j.tibs.2010.07.003

34. Bhat AH, Dar KB, Anees S, Zargar MA, Masood A, Sofi MA, Ganie SA (2015) Oxidative stress, mitochondrial dysfunction and neurodegenerative diseases; a mechanistic insight. Biomed Pharmacother 74:101–110. https://doi.org/10.1016/j.biopha.2015.07.025

35. Kwiatkowski TJ, Bosco DA, Leclerc AL, Tamrazian E, Vanderburg CR, Russ C, Davis A, Gilchrist J et al (2009) Mutations in the FUS/TLS gene on chromosome 16 cause familial amyotrophic lateral sclerosis. Science 323(5918):1205–1208. https://doi.org/10.1126/science.1166066

36. Howland DS, Liu J, She Y, Goad B, Maragakis NJ, Kim B, Erickson J, Kulik J et al (2002) Focal loss of the glutamate transporter EAAT2 in a transgenic rat model of SOD1 mutant-mediated amyotrophic lateral sclerosis (ALS). Proc Natl Acad Sci U S A 99(3):1604–1609. https://doi.org/10.1073/pnas.032539299

37. Ruffoli R, Bartalucci A, Frati A, Fornai F (2015) Ultrastructural studies of ALS mitochondria connect altered function and permeability with defects of mitophagy and mitochondriogenesis. Front Cell Neurosci 9:341. https://doi.org/10.3389/fncel.2015.00341

38. Golpich M, Amini E, Mohamed Z, Azman Ali R, Mohamed Ibrahim N, Ahmadiani A (2017) Mitochondrial dysfunction and biogenesis in neurodegenerative diseases: pathogenesis and treatment. CNS Neurosci Ther 23(1). https://doi.org/10.1111/cns.12655

39. Kodavati M, Wang H, Hegde ML (2020) Altered mitochondrial dynamics in motor neuron disease: an emerging perspective. Cells 9(4). https://doi.org/10.3390/cells9041065

40. Zhou J, Li A, Li X, Yi J (2019) Dysregulated mitochondrial Ca and ROS signaling in skeletal muscle of ALS mouse model. Arch Biochem Biophys 663:249–258. https://doi.org/10.1016/j.abb.2019.01.024

41. Petersen KF, Befroy D, Dufour S, Dziura J, Ariyan C, Rothman DL, DiPietro L, Cline GW et al (2003) Mitochondrial dysfunction in the elderly: possible role in insulin resistance. Science 300(5622):1140–1142. https://doi.org/10.1126/science.1082889

42. Carrière A, Carmona M-C, Fernandez Y, Rigoulet M, Wenger RH, Pénicaud L, Casteilla L (2004) Mitochondrial reactive oxygen species control the transcription factor CHOP-10/GADD153 and adipocyte differentiation: a mechanism for hypoxia-dependent effect. J Biol Chem 279(39):40462–40469. https://doi.org/10.1074/jbc.M407258200

43. Pu J, Ha CW, Zhang S, Jung JP, Huh W-K, Liu P (2011) Interactomic study on interaction between lipid droplets and mitochondria. Protein Cell 2(6):487–496. https://doi.org/10.1007/s13238-011-1061-y